

## Research Article

# Computer 5G Virtual Reality Environment 3D Clothing Design

**Huabai Liu** 

*College of Art and Design, Hunan Automotive Engineering Vocational College, Zhuzhou, 412001 Hunan, China*

Correspondence should be addressed to Huabai Liu; [liuhuabai2021@163.com](mailto:liuhuabai2021@163.com)

Received 18 January 2022; Revised 21 February 2022; Accepted 4 March 2022; Published 23 March 2022

Academic Editor: Chia-Huei Wu

Copyright © 2022 Huabai Liu. This is an open access article distributed under the Creative Commons Attribution License, which permits unrestricted use, distribution, and reproduction in any medium, provided the original work is properly cited.

With the increasing computing power of computer hardware and the continuous development of Internet technology, it has become possible to sell clothing online. In this context, virtual clothing shops and fitted clothing have also started to appear online and people have a new platform to choose their clothing. In the development of the clothing industry, e-tailoring will become a new trend, and if we look at the clothing industry as a whole, e-tailoring is bound to develop rapidly, as it is now difficult for people to find clothes they are happy with on the shelves. However, many clothing shops on online platforms are now able to provide a more limited service to people, making it difficult for consumers to buy the right clothes for them, and the situation of returns is more serious. So many consumers are still more willing to buy clothes in the physical shop; if we can use the virtual reality environment of three-dimensional clothing design, consumers in the online clothing shop can freely choose their favorite clothing, and then the selected clothing considers the proposed wear in accordance with the size of the consumer production of the human body virtual model to observe the three-dimensional effect so that consumers can choose more suitable clothing. This paper mainly studies the 3D clothing design method in the computer 5G virtual reality environment. In the context of the computer 5G era, this article discusses the characteristics of virtual reality technology in detail and proposes a modeling method for 3D clothing design based on virtual reality. Based on the research status of 3D clothing design at home and abroad, this paper further studies the construction of clothing virtual design and designs and realizes the functions of character virtual modeling, clothing virtual modeling, and accessory virtual modeling. According to the defects of the existing 3D clothing design, a more mature three-dimensional clothing design method based on actual needs is developed. This paper analyzes the 3D clothing design process in detail through demand analysis; constructs the system functional block diagram, system architecture diagram, style customization flowchart, database table, etc.; designs the 3D clothing design module; and designs the main clothing and portraits—part of the modeling. Experimental studies have found that as long as  $|Z| > 0.042547$  is satisfied, the clothing and the human body part can be prevented from crossing when the clothing matches the human body. In this article, in order to prevent large deviations in the garment stitching process, if it is the front piece of the garment, take  $Z = 0.06$ . If it is the back film, take  $Z = -0.06$ . Virtual reality technology-assisted clothing design has become a new model of computer-aided clothing design, which has successfully promoted the transformation of enterprise employment forms and the improvement of enterprise production efficiency. The percentages of the left neck point, right neck point, left hip point, and right hip point in the human feature points were 15%, 23%, 31%, and 31%, respectively.

## 1. Introduction

With the continuous development of today's virtual reality technology, the clothing industry is also undergoing earth-shaking changes. Technologies such as three-dimensional clothing design, intelligent clothing panel making, and clothing computer-aided design are gradually developing in the clothing field. Nowadays, 3D clothing design technology

has been widely used in the fields of medicine, simulation, human body modeling, and 3D animation. In the clothing industry, the traditional body size measurement method is based on manual measurement, and its efficiency is low. The data obtained is often different due to human emotions, measurement methods, technology, and many other factors, which affect body measurement. The accuracy of the data is bound to have a certain impact on the later garment

production and processing. How to obtain the key dimensions of human clothing design more scientifically, conveniently, accurately, and quickly is particularly important for the development of the clothing industry.

The virtual clothing collocation technology is the product of the combination of computer technology and clothing. It is no longer the same as the manual mode in the past to make patterns but directly according to actual needs, in accordance with the general matching principles in the computer system such as color sample matching and style matching, combining different materials, different styles, and different color designs in ways such as style matching [1, 2]. The clothing virtual collocation system is to realize the virtual collocation technology so that the technology can be used in the computer system to choose the matching of different clothing so that the user can know the final effect in advance before the actual production design of the clothing and modify the unsatisfactory details—speed of response to winning the market [3].

At present, the research enthusiasm for three-dimensional clothing design continues. In order to meet the needs of personalized clothing customization, Zhu et al. proposed interactive clothing design and a personalized virtual display with the user's own face. Taking suits as an example, the method of customer interactive clothing design based on genetic engineering ideas is analyzed. Therefore, customers can rearrange clothing style elements, choose available colors and fabrics, and propose their own personalized suit styles. Based on Unity3D and VR technology, they developed a Web3D customized prototype system for personalized clothing. The structure and function layout combined with the system flow are given. But it did not solve practical problems such as 3D facial scanning, suit style design, fabric selection, and accessory selection [4]. Chen et al. took typical Tibetan costumes and traditional Chinese costumes as examples and proposed a virtual reality interactive teaching mode for clothing design education. These processes include the use of two-dimensional (2D) clothing CAD software to display traditional clothing structures, the use of virtual reality technology to make three-dimensional (3D) clothing models, and the use of the Unity3D game development platform for interaction [5]. Sun et al.'s research investigated the first and second air gaps under the garment and also tested the thermal performance related to the microclimate volume formed between the garment layers forming the whole. For outerwear, there is no threshold volume determined, after which the insulation layer will start to decrease due to convection. Use accurate 3D body scans and CAD tools to reverse-engineer the process to assess the volume of microclimate air. The thermal human body model was used to examine the influence of the microclimate volume on the overall thermal insulation material, which was used for outerwear [6]. Kang et al. have developed an advanced three-dimensional (3D) human body temperature regulation model to describe the temperature distribution across the skin surface and body. In the model, the human body is divided into 15 parts, and the geometry of the limbs is modeled as a frustoconical shape to imitate the physical geometry of the upper arm, forearm, thigh, and calf

[7]. Yang et al. presented a novel waist measurement system based on multiview stereo images for garment design. The system is set up at a fixed location and captures three pairs of stereo images for the subject through six calibrated and synchronously triggered cameras. The maximum measurement error of the system was 1.28 cm for women and 1.31 cm for men for bust measurement and 1.18 cm for women and 0.99 cm for men for waist measurement, both within the error limits set by the Chinese national and textile industry standards [8].

The main innovations of this paper include the following aspects. (1) Propose a new three-dimensional cutting method, using virtual reality technology to calculate and deform each point of the characteristic part of the model separately; the characteristic part transitions naturally, and the modeling effect is more realistic. Use the three-dimensional B-spline technology to establish a clothing universal type, and complete the clothing design process by making changes to the clothing universal type, which is convenient to operate and avoids repeated labor. (2) Based on the constant distance from the center key point to the boundary key point before and after the 3D garment is expanded, a geometric expansion algorithm based on the calculation of the length of the 3D B-spline curve is proposed. (3) This paper observes the 3D effects of designing garments in a virtual reality environment. The 3D interactive sphere enables the spatial control of 3D objects with 6 degrees of freedom and, through it, the design of 3D virtual garments.

## 2. Three-Dimensional Clothing Design in Virtual Reality

Clothing design belongs to the category of arts and crafts, and it is an art form that combines practicality and artistry. Design means planning, conceiving, and setting up plans. It also includes imagery, drawing, and modeling. The definition of clothing design is a creative plan and creative behavior that solves the problems in people's wearing life system. It is a marginal subject involving a wide range of fields and is closely related to social sciences and natural sciences such as literature, art, history, philosophy, religion, aesthetics, psychology, physiology, and ergonomics. As a comprehensive art, costume design has the common characteristics of general practical art, but it also has its own characteristics in content, form, and means of expression. Figure 1 shows Dali's "Lobster Skirt" and Dali's "Eternal Eye Brooch."

Nowadays, clothing is no longer simply a tool for people to conceal the body but a medium and symbol to convey personal personality and a cultural carrier that integrates artistry, functionality, and emotion. If the designer is stuck in the inherent concept for a long time, it means that the inspiration is exhausted.

In today's general environment, cross-border thinking combines many artistic fields to make the design unique and full of freshness. As a weather vane of the trend, clothing will inevitably be affected by it, and cross-border clothing has emerged as the times require. Andy Warhol is known as one of the most influential figures in the art world in the 20th century. He is the iconic artist of Pop Art and the



FIGURE 1: Dali's works.

artist who has the greatest influence on Pop Art. He boldly uses unconventional methods such as letterpress printing, rubber or wood rubbing, gold foil technology, and photo projection in his artistic creations. His artistic style is diversified, and his works are full of practicality, commerciality, and humor. Andy Warhol had close contact with celebrities in the fashion circle during his lifetime. Many photographers, models, and celebrities at the time were his good friends. In fact, the starting point of his career was to paint costume illustrations for the American version of “Bazaar,” which was different from the later painting styles. The illustrations at that time were mainly based on simple lines. Andy Warhol became famous in New York and became the most popular illustrator at the time. In his early illustrations, a creative object that cannot be ignored is women’s high-heeled shoes. The image of high-heeled shoes frequently appears in his manuscripts. The bold color matching and gorgeous prints of the shoes have inspired countless designers and derived subsequent works, as shown in Figure 2.

In the design of clothing with Hanfu elements, what is expressed is a Chinese cultural sentiment, which is transformed from abstract to figurative, the elements of which are decomposed, added or subtracted, and integrated into contemporary clothing design, fusing the plot of Hanfu elements into the clothing to be designed. In this process of integration, their products not only reflect the designer’s special attachment to traditional Chinese culture and its carriers but also present the viewer with a stylish and creative look and feel with elements of Hanfu culture.

**2.1. 5G Network Architecture.** The 4G network cannot cope with the 5G requirements and scenarios on the network due to the limitations of its access network technology and the solidification of network architecture functions. In contrast, 5G networks have faster speeds, better communication quality, and more diverse service scenarios, which can make 5G networks more efficient through technological innovation and coordinated development in both infrastructure platforms and network architecture—flexible, intelligent, and open [8, 9]. In terms of infrastructure platforms, 5G networks introduce NFV and SDN technologies and build new platforms on the same set of hardware facilities, thereby reducing the cost of existing infrastructure platforms,

enhancing resource management capabilities, and accelerating service launches. In terms of network architecture, the network architecture is redesigned by combining the technologies of control forwarding separation and control function reconstruction to improve the performance of the access network (AN) in the 5G scenario. In addition, the simplified core network (CN) structure makes the control forwarding function more flexible and efficient, the operation is more intelligent, and the network capability is more open so that the overall service level of the entire network is improved [10].

The new 5G network architecture includes three functional planes: access, control, and forwarding. The control plane generates a global control strategy, which is then executed by the access plane and the forwarding plane. The access plane includes various types of base stations and wireless access devices. The increasingly powerful interaction capabilities and diversified networking topologies between base stations make coordinated wireless access control more flexible and improve the utilization of wireless resources. The control plane recombines network functions, centralizes control functions, simplifies control procedures, and realizes flexible scheduling of the access and forwarding resources [11, 12]. The network functions are arranged according to the needs of different services to realize the customization of network resources and the openness of network capabilities. The forwarding plane includes distributed gateways with sinking user planes, integrating edge data caching and service acceleration functions, and improving data forwarding efficiency and flexibility under the centralized control of the control plane [13, 14]. The application areas of 5G are shown in Figure 3.

The design process of the access network requires attention to the following: (1) the allocation of virtual resources through the base station and the possibility of processing the baseband through SDR, as well as the shift to virtualized base stations with real-time cloud architecture; (2) the convergence of 2G, 3G, 4G, and Wi-Fi access technologies; (3) the content caching and delivery at the edge and the transfer to the access network to the traditional mobile network content storage and distribution functions, according to the actual needs of users to push information at times, so as to continue to improve the user experience; and (4) the flattening of the data plane and optimization of data transmission



FIGURE 2: Andy Warhol's design manuscript.

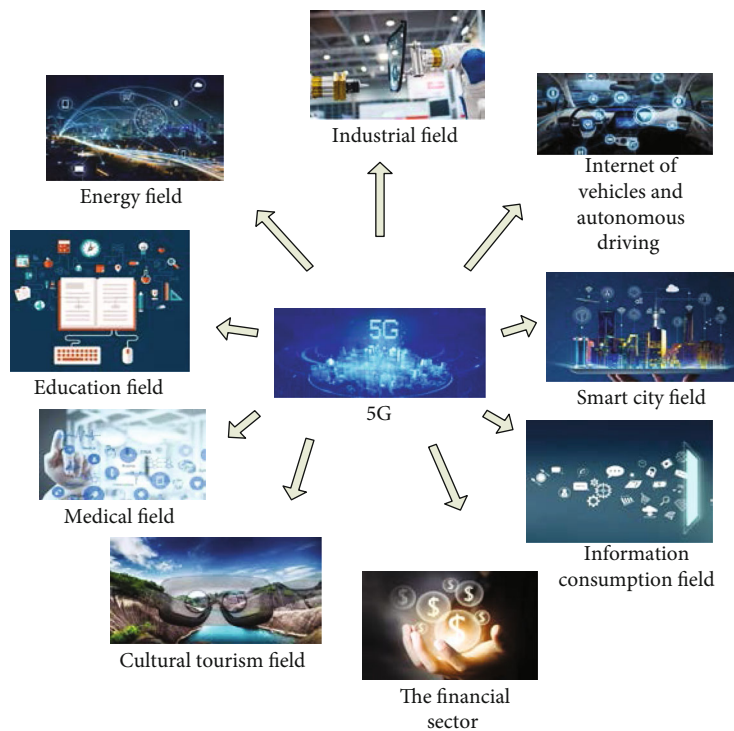


FIGURE 3: 5G application areas.

paths. The data plane is flattened, and the data transmission path is optimized.

For virtual reality technology has many technical characteristics, mainly including perceptibility, presence, and other related technologies, the computer graphic image in the design process combined with the virtualized element image, in the elements of the most important element, is the effect of immersion. The perceptual system itself is an effective way of targeting the visual instincts of the graphic image elements to effectively increase immersion as the viewer carries out both the virtual and realistic dimensions for observation. On this basis, the design of computer graphics must have a perceptual effect that aids immersion. This is what makes it possible to achieve a visual approximation to reality. Therefore, to be able to design the effect of computer graphic images, virtualization and immersion should be the main

premise, constantly enriching the design principles of graphics and complementing the content of images, so that the visual effect of virtual reality technology can be effectively brought into play.

2.2. *Virtual Reality Technology.* Virtual reality, VR for short, has been a popular field in recent years in the field of computer networks and related fields. It is a high-tech development involving many disciplines in the 20th century. Virtual reality technology is a technology developed on the basis of computer graphics, computer simulation technology, human-computer interface technology, multimedia technology, and sensor technology [15, 16]. VR technology is a computer-generated data map of simulated stereo vision. People have a specific real world without recognition results or show a purely conceived world. People use data gloves,

data clothes, and other sensing devices to input data and obtain the corresponding visual, auditory, and tactile sensations so as to achieve the closest interaction with the natural state of this reproduced world [17]. Nowadays, VR technology is actively used in entertainment, audiovisual arts, military training, aerospace, and other fields. The ideal virtual reality technology is to create a virtual environment through a computer, using human vision, hearing, touch, taste, smell, and other functions to make people feel the same as reality, have an immersive feeling, and achieve the interaction between the user and the environment. The mainstream VR equipment is shown in Figure 4.

Because virtual technology is used in the process of automating the computer, this technology is closely related to the design technology of graphic images. To a certain extent, it gives a feeling of immersion. But the designers are mainly combining virtual and realistic technologies for effective coordination and control in their specific designs and are able to present people in a realistic way through three-dimensional technology, thus allowing friendly human-computer interaction.

Virtual reality technology has three basic characteristics: immersion, interaction, and imagination. Immersiveness refers to the criticality of the user's integration into reality. The interaction between humans and machines is natural, just like the interaction between humans and nature in reality, completely immersed in the virtual environment [18, 19]. Interactivity is different from the playback of 3D scenes and realizes human-computer interaction through human sensory organs instead of passive acceptance. Conception means that through this system, users can get perceptual and rational knowledge and thus have a new understanding and perception of a certain thing [20]. The application areas of VR are shown in Figure 5.

**2.3. Three-Dimensional Cutting Technology.** Three-dimensional cutting is a method of cutting and creating directly based on the human body according to the needs of the design. It is not restricted by the plane calculation formula and empirical data. The operator can directly perceive the shape and characteristics of the human body. It is a very simple and the most intuitive way to make clothing [21, 22]. The three-dimensional cutting method of making clothes eliminates the design steps of paper patterns and is a very intuitive way to show the relationship between the human body shape and the clothing composition. Three-dimensional clothing cutting is also called three-dimensional clothing design. The structure design of non-clothing plane cutting is the most primitive and fundamental form of clothing structure design. It pursues the perfect combination of technology and art, the combination of clothing and the human body, and the combination of fabrics and shapes [23]. Three-dimensional cutting is the understanding and application of designers and pattern makers on the aesthetics of clothing art. It mainly uses a human table, scissors, pins, fabrics, and other tools and materials to actually operate on the human table. The structure, shape, and silhouette of the clothing are all around, produced in the three-dimensional space of the human plat-

form. The specific operation is as follows: cover the human table with a white-grey cloth; fix it with a pin; directly use the processing methods such as saving, dividing, and pleating by hand to produce the expected clothing art style; and use the marking line to clearly mark the modeling structure line. Finally, the fabric of the human table is removed, cut, and sew into a sample garment, which is tried on by the human body, and the unsuitable parts of the trial fitting are modified, and the modified parts are clearly marked with the marking line, and finally, a sample garment that meets the needs of the human body is obtained. Split the fake sewing pieces, and then spread them on paper to make a conventional clothing pattern [24, 25]. With this form of making clothing, you can intuitively see the effect of the clothing during the production process, and you can improve and adjust the plan at any time. Throughout the classic and creative clothing styles of international brands, it is all reflected in the three-dimensional cutting mode. The effect design diagram is shown in Figure 6.

In the three-dimensional clothing design, the generation and sewing of clothing pieces is a very important link. This link mainly contains two reverse processes. The first is the cutting piece from the two-dimensional to the three-dimensional visual mapping process; in this process, it needs to be sewn on the three-dimensional human body model on the two-dimensional clothing cut pieces so as to be able to form a three-dimensional clothing initial form. The second is the entire clothing piece or entire cutting process, which is the two-dimensional unfolding process of the three-dimensional clothing surface, which requires the three-dimensional clothing surface to be unfolded into the prescribed two-dimensional flat type, thus forming the two-dimensional cutting piece required for clothing processing. The process of generating and sewing garment pieces is now largely carried out using unfolding techniques. Some designers see the three-dimensional visualization of their garment pattern as a purely geometric problem, triangulating the two-dimensional pattern and then mapping the layers onto the three-dimensional mannequin: the three-dimensional surface is a more complex process in the production of the two-dimensional pattern.

**2.4. Three-Dimensional B-Spline Technology.** Since this article designs three-dimensional clothing modeling technology, it is inseparable from three-dimensional curve modeling, and three-dimensional curve modeling is based on two-dimensional curve modeling: the positive seeking process and control point inverse process of the B-spline curve. The key technology of this article will be explained in this section. The equation of the B-spline can be written as

$$p(u) = \sum_{i=0}^n d_i N_{i,k}(u). \quad (1)$$

It can be seen from the equation that in order to obtain a B-spline curve, a series of control points and corresponding B-spline basis functions must first be provided. Now, suppose that a number of control points on a curve are known;



FIGURE 4: VR equipment.

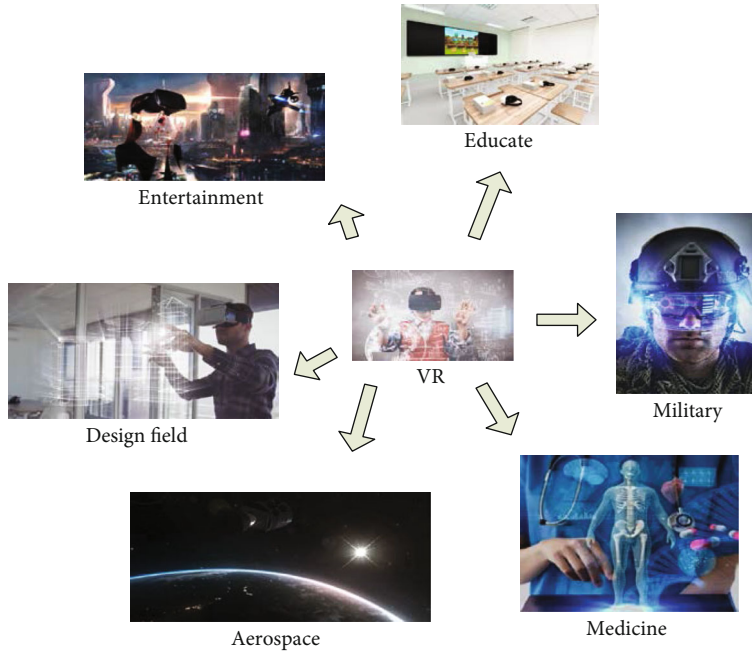


FIGURE 5: Application areas of VR.

then, what needs to be solved now is the corresponding B-spline basis function part. The Debre-Cox recurrence formula used here is

$$\begin{cases} N_{i,0}(u) = \begin{cases} 1, & u_i \leq u \leq u_{i+1}, \\ 0, & \text{other} \end{cases} \\ N_{i,k}(u) = \frac{u - u_i}{u_{i+k} - u_i} N_{i,k-1}(u) + \frac{u_{i+k+1} - u}{u_{i+k+1} - u_{i+1}} N_{i+1,k-1}, \\ \frac{0}{0} = 0. \end{cases} \quad (2)$$

It can be seen from the formula that to solve the B-spline base  $N_{i,k}$ , a corresponding node sequence must be obtained first. To sum up, what is known is the group of control points, and what I want to solve is the entire B-spline curve. To solve the B-spline curve, the node sequence of the curve

must be obtained first, so the node sequence of the curve must be solved through this set of known control points. The calculation of the two node sequences introduced in this article is also based on this principle to parameterize the chord length [26].

The first introduced is the Liesenfeld method. The control polygon (that is, the polygon formed by sequentially connecting the control points) is approximately regarded as the circumscribed polygon of the curve, and the segmented connection points of the curve correspond to the vertices or edges that control multideformation. Then, the chord length of each segment of the curve is regarded as the sum of the corresponding side lengths of the corresponding control multideformation, and then the total side length of the polygon is the quotient to obtain the value of the normalized node sequence [27, 28]. Due to the different properties of odd-order spline functions and even-order spline functions, their solution methods are also different. Liesenfeld assumes that the segment connection points of the even-order B-spline curve correspond to the midpoints

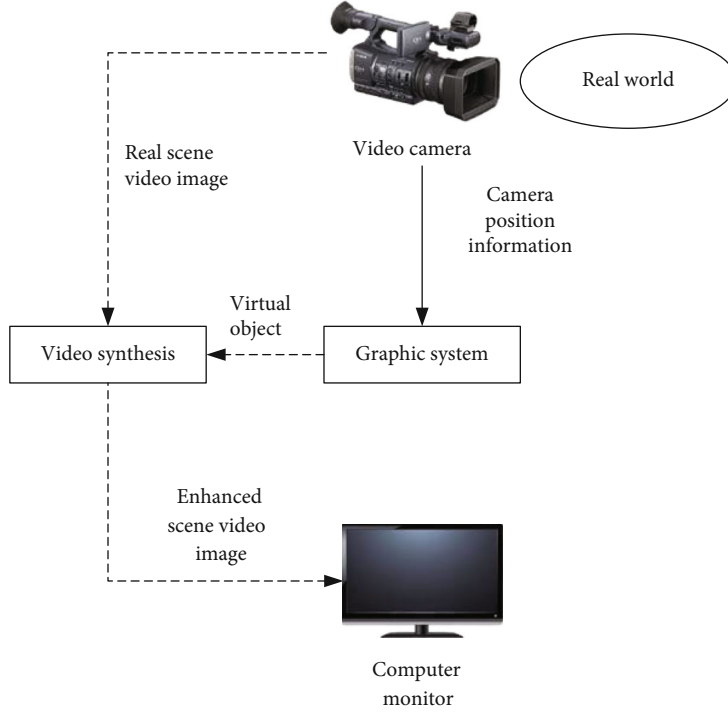


FIGURE 6: Effect design drawing.

of the control multideformation, but this correspondence should remove the  $k/2$  sides at both ends of the control

polygon [29, 30]. Therefore, the node sequence can be obtained as

$$U = 0, 0, \dots, \frac{\left(\sum_{j=1}^{k/2} l_j\right) + \left(l_{(k/2)+1}/2\right)}{L}, \frac{\left(\sum_{j=1}^{(k/2)+1} l_j\right) + \left(l_{(k/2)+1}/2\right)}{L}, \dots, \frac{\left(\sum_{j=1}^{n-(k/2)-1} l_j\right) + \left(l_{n-(k/2)}/2\right)}{L}, 1. \quad (3)$$

At the same time, Liesenfeld assumes that the segmented connection points of the odd-order B-spline curve correspond to the  $nk$ -th control point. This correspondence is that  $(k+1)/2$  at both ends of the control multideformation are removed, established after the vertex. Then, expand, sum, and normalize it to get its node sequence, namely,

$$U = 0, 0, \dots, 0, \frac{\sum_{j=1}^{(k+1)/2} l_j}{L}, \frac{\sum_{j=1}^{((k+1)/2)+1} l_j}{L}, \dots, \frac{\sum_{j=1}^{n-((k+1)/2)} l_j}{L}, 1. \quad (4)$$

**2.5. Geometric Operations of Implicit Surfaces and Implicit Functions.** The low-dimensional interface in the three-dimensional space is a curved surface, which divides the three-dimensional space into isolated nonzero subregions. Here, we only consider closed surfaces that can clearly distinguish between the inside and the outside. For example, consider the following expression:

$$\lambda(\vec{a}) = a^2 + b^2 + c^2 - 1. \quad (5)$$

In this expression, the interface passes

$$\lambda(\vec{a}) = 0. \quad (6)$$

For the definition of the isosurface, the interface is also a unit sphere:

$$\partial\Delta = \left\{ \vec{a} \mid \|\vec{a}\| = 1 \right\}. \quad (7)$$

For the surface, the inner area is

$$\Delta^- = \left\{ \vec{a} \mid \|\vec{a}\| < 1 \right\}. \quad (8)$$

The outer area is

$$\Delta^+ = \left\{ \vec{a} \mid \|\vec{a}\| > 1 \right\}. \quad (9)$$

The explicit expression of the interface is

$$\partial\Delta = \left\{ \vec{a} \mid \left| \frac{\vec{a}}{|\vec{a}|} \right| = 1 \right\}. \quad (10)$$

For complex surfaces without analytical expressions, we also need to discretize the surface. It is difficult to discretize explicit expressions in three-dimensional space. We need to select a large number of points on the two-dimensional surface and record their connectivity. In two-dimensional space, connectivity is usually determined by order; that is,  $\vec{a}(s_i)$  is connected with points  $\vec{a}(s_{i-1})$  and  $\vec{a}(s_{i+1})$ . The representation of connectivity in three-dimensional space is far from straightforward. If you know a certain precise surface and its connectivity, the surface can be easily drawn from the triangle surface, where the vertices of the triangle surface are on the surface, and the edges of the triangle surface indicate the connectivity. On the other hand, if you do not know the connectivity, it will be difficult to draw the surface correctly. Even if you use a very well-known algorithm, the drawn surface will have many strange errors, such as a surface with holes.

Another advantage of the implicit level set representation of space is that it is easy to perform Boolean operations and solid drawing geometric operations. For example, given  $\lambda_1$  and  $\lambda_2$ , we can easily perform the following operations:

$$\lambda = \max(\lambda_1, \lambda_2), \quad (11)$$

$$\lambda = \min(\lambda_1, \lambda_2), \quad (12)$$

$$\lambda = \max(\lambda_1 - \lambda_2). \quad (13)$$

The definition of the distance function is as follows: for all  $\vec{a}_1 \in \Gamma$ ,

$$d(\vec{a}) = \min \left( \left| \vec{a} - \vec{a}_1 \right| \right). \quad (14)$$

It can be seen from the definition that when the unknown point is on the boundary, the function value is 0. From a geometric point of view,  $d$  can be considered to be obtained by the following method: if  $\vec{a} \in \Gamma$ , then  $d(\vec{a}) = 0$ , for some other given point  $\vec{a}$ ; find the point closest to  $\vec{a}$  on the boundary, and mark the closest point as  $\vec{a}_z$ ; the value of the distance function is

$$d(\vec{a}) = \left| \vec{a} - \vec{a}_z \right|. \quad (15)$$

For a given point  $\vec{a}$ , assuming that  $\vec{a}_z$  is the point closest to  $\vec{a}$  on the interface, for any point  $\vec{b}$  on the line segment connecting points  $\vec{a}$  and  $\vec{a}_z$ ,  $\vec{b}$  is also the point closest to  $\vec{a}$  on the interface. From the definition of the distance function, the specific definition of the signed distance function can be obtained as

$$\lambda(\vec{a}) = d(\vec{a}) = 0, \quad \vec{a} \in \Gamma, \quad (16)$$

$$\lambda(\vec{a}) = -d(\vec{a}), \quad \vec{a} \in \Delta^-, \quad (17)$$

$$\lambda(\vec{a}) = d(\vec{a}), \quad \vec{a} \in \Delta^+. \quad (18)$$

The signed distance function is a subset of the implicit function and has all the properties of the implicit function discussed in the previous section. The signed distance function can simplify many level set methods for dealing with implicit functions. Its additional attribute similar to the distance function is  $|\nabla\lambda| = 1$  so that the unit normal vector does not need to be normalized.

The main idea of the level set method is to define the moving interface as the zero isosurface of a function, and let the function move at an appropriate speed so that the zero isosurface is the material interface. At any time, as long as you know the function and find its zero isosurface, you will know the active interface at this time. The symbolic distance function defined in the previous section conforms to the idea of the level set function and has many excellent characteristics, so we generally choose the symbolic distance function as the level set function in the experiment; that is, the definition of the level set function is as follows:

$$\lambda(\vec{a}) = d(\vec{a}), \quad \vec{a} \in \Delta^+, \quad (19)$$

$$\lambda(\vec{a}) = d(\vec{a}) = 0, \quad \vec{a} \in \Gamma, \quad (20)$$

$$\lambda(\vec{a}) = -d(\vec{a}), \quad \vec{a} \in \Delta^-. \quad (21)$$

After defining the level set function, the motion of the interface depends on the velocity field  $\vec{u}$ , which may be related to many factors, such as the location, time, temperature, geometric characteristics of the interface, or external force applied to the interface. After defining the velocity field, the following level set equation can be obtained:

$$\lambda_1 + \vec{u} \cdot \nabla\lambda = 0. \quad (22)$$

In order to improve the efficiency of the algorithm, the equation only needs to be solved in the local area near the interface.

For the function value and velocity field of the level set function, if the interleaved MAC method is used, the specific storage methods in two-dimensional and three-dimensional spaces are shown in Figures 7 and 8, respectively.

If the MAC method is used to store data, the data storage mode of a grid unit in the two-dimensional space is shown in Figure 9.

This paper chooses the staggered MAC grid method to store data because it can calculate unbiased "central difference," such as pressure gradient and velocity divergence, so as to avoid some common defects. This advantage is illustrated by the following example. In order to be more general, we consider the situation in a one-dimensional space. Now, suppose there is a set of one-dimensional data  $q$ , which are discretely sampled at grid positions  $1, 2, 3, \dots, i-1, i, i+1,$



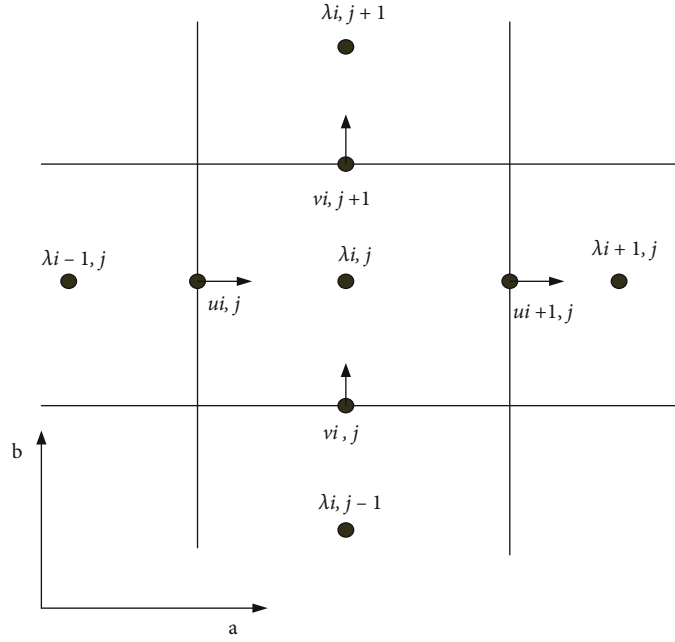


FIGURE 7: Interleaved MAC storage method of data in a two-dimensional grid.

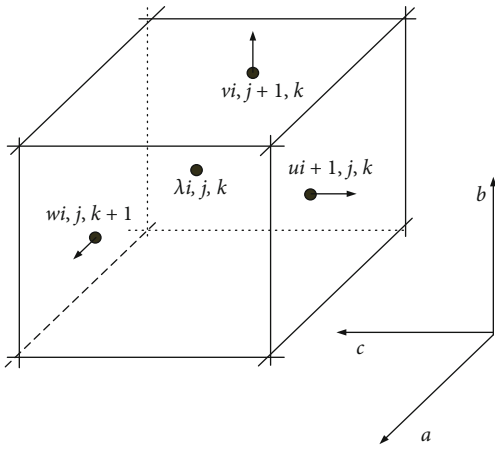


FIGURE 8: Interleaved MAC storage method of data in a three-dimensional grid.

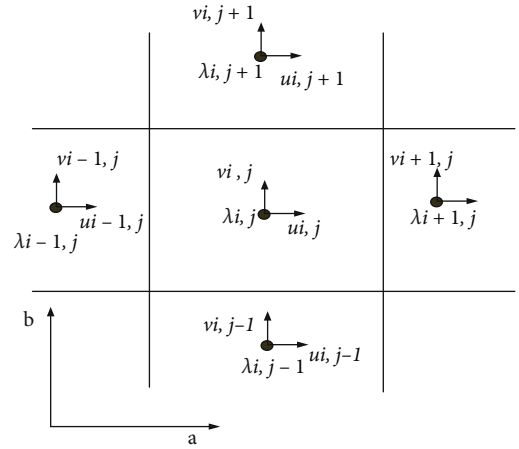


FIGURE 9: MAC storage method of data in a two-dimensional grid.

..., and their sampling values are  $q_1, q_2, q_3, \dots, q_{i-1}, q_i, q_{i+1}$ , and what is to be calculated is the derivative value  $(\partial q / \partial a)_i$  at grid cell  $i$ . In order to avoid deviation as much as possible, the commonly used difference method is

$$\left(\frac{\partial q}{\partial a}\right)_i \approx \frac{q_{i+1} - q_{i-1}}{2\Delta a}. \quad (23)$$

This method not only has no directional deviation, but the error is also a second-order  $O(\Delta a^2)$ . And another difference method is

$$\left(\frac{\partial q}{\partial a}\right)_i \approx \frac{q_{i+1} - q_i}{\Delta a}. \quad (24)$$

The method used will have a deviation to the right because when calculating the difference, only the right-side value is considered and the left-side value is ignored, and the numerical error is only  $O(\Delta x)$ . What kind of difference format can not only guarantee the second-order accuracy but also avoid the directional deviation and zero space problems? The solution is to use the storage scheme of the staggered MAC grid: the value  $q$  at the grid unit  $i$  is not sampled, and the sampling network is used instead of the value  $q_{i+1/2}$  at half of the cell. Then, when calculating the derivative value at grid cell  $i$ ,

$$\left(\frac{\partial q}{\partial a}\right)_i \approx \frac{q_{i+1/2} - q_{i-1/2}}{\Delta a}. \quad (25)$$

In addition, knowing the normal component of the

center velocity on each surface of each grid unit, we can easily calculate the divergence  $\nabla \cdot \vec{u}$  of the flow field.

### 3. 3D Clothing Design Modeling Experiment

**3.1. Experimental Platform.** The laser is used to perform noncontact appearance scanning of the object to obtain point data, which can be quickly formed after postprocessing, with the 3D solid model showing a simple loose-fitting top T-shirt [31, 32]. 3D virtual reality technology is different from pure surveying and mapping technology. It is mainly for high-precision inverse 3D modeling and reconstruction. Traditional measurement technology is mainly single-point accurate measurement, but it is not suitable for modeling work because it is described. The complete properties of the target structure require a large number of surveying and mapping points, ranging from tens of thousands to more than several million so that the target can be completely moved to the computer [33]. Using modern high-precision sensing technology as an aid to solve this problem, three-dimensional virtual reality technology is this kind of automatic high-precision stereo scanning technology. The system design and system flow are shown in Figures 10 and 11.

#### 3.2. Experimental Procedure

**3.2.1. Basic Information and Exercise Habits.** The subjects fill in the questionnaire about basic information and exercise habits. If they have not used the virtual somatosensory game, they will first use the game to play for an hour and be familiar with the operation method of the virtual somatosensory game.

**3.2.2. Actual Scene Test.** First of all, the subjects put on sports clothing to measure their weight and were not allowed to drink water or add or remove clothing during exercise. During this period, the blood pressure of the subject's left wrist was measured, and the diastolic blood pressure (DBP) and systolic blood pressure (SBP) were recorded, respectively. After that, an alcohol cotton ball was used to clean the fingertips of the subjects. Squeeze your fingers and measure the blood lactic acid value of the subject before exercise with the blood lactic acid test paper. The humidity values under the front of the chest, under the back, under the left armpit, and under the right underarm were measured with a hygrometer. The subjects undressed and photographed the upper body surface temperature, taking the front chest body surface temperature, back body surface temperature, left armpit body surface temperature, and right armpit body surface temperature. After the subjects wear the heart rate monitor on their chest, they are set to record their heart rate every 2 s (the heart rate is recorded every 2 s below). The subjects put on sports clothing, performed a 30-minute actual scene test in an indoor sports field, and recorded their heart rate at the beginning of the exercise. After 30 minutes of exercise, stop recording the heart rate. In the same step, the test subject's weight after the actual scene test exercise was measured. Record the diastolic blood pressure DBP2;

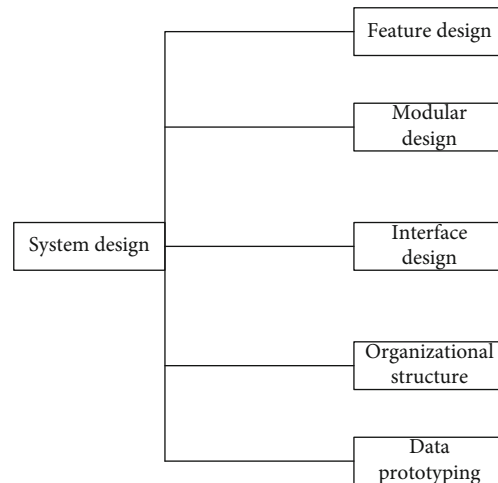


FIGURE 10: System design diagram.

systolic blood pressure SBP2; blood lactate LAC; humidity under the clothes of the front chest, back, left armpit, and right armpit; and body surface temperature of the front chest, back, left armpit, and right armpit. The subjects filled out a questionnaire for subjective evaluation of sportswear comfort in the actual scene test. Then, sit and rest for half an hour.

**3.2.3. Virtual Scene Test.** In the same step (Section 3.2.2), record the test subjects' weight before the virtual scene test exercise; diastolic blood pressure DBP3; systolic blood pressure SBP3; blood lactic acid LAC; humidity under the front chest, back, left armpit, and right armpit; and body surface temperature on the front chest, back, left armpit, and right armpit. The subjects put on a heart rate monitor, used games in the laboratory to perform a 30-minute virtual scene test, and recorded their heart rate at the beginning of the exercise. After 30 minutes of exercise, stop recording the heart rate. The test subjects in the same step (Section 3.2.2) test the body weight of the virtual scene after exercise; the diastolic blood pressure DBP4; the systolic blood pressure SBP4; the humidity of the front chest, back, left armpit, and right armpit; and the body surface temperature of the front chest, back, left armpit, and right armpit. The subjects filled out a questionnaire for subjective evaluation of sportswear comfort in the virtual scene test.

**3.3. Data Collection.** Import the established standard model into 3DS MAX, slice it, retain its main body, and merge all body parts into one object. Then, export the model data to the file Women ASE. Before exporting, set the data accuracy to two decimal places, and other settings are default. This file contains all the mesh and vertex information of the model. Export the ASE file, which means that the original data required for human platform modeling has been obtained. But in order to draw the human platform model, it must first be read and stored through programming. After the reading is completed, it is finally drawn through the OpenGL graphic interface.

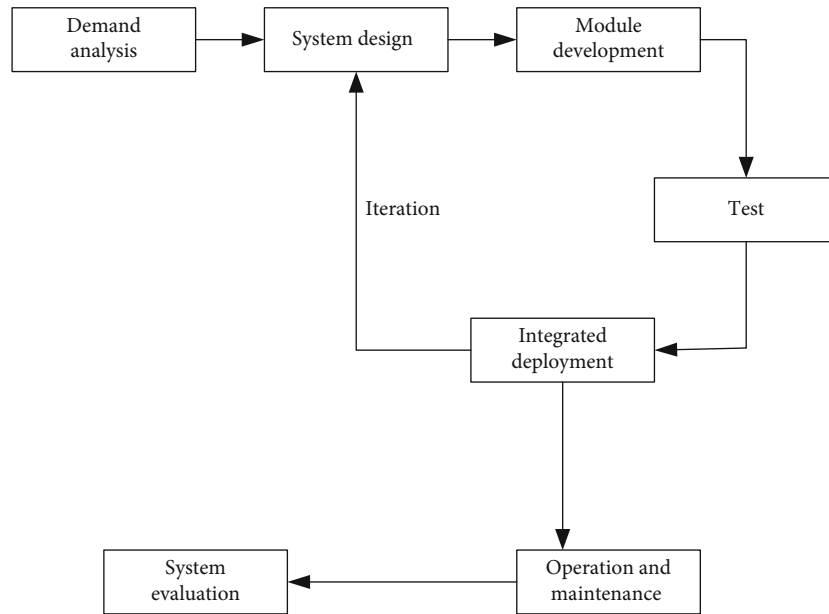


FIGURE 11: System design research flowchart.

### 4. Three-Dimensional Clothing Design Data Analysis

4.1. *Comparative Analysis between Three-Dimensional Cutting and Different Clothing Shapes.* Analyze the results from the main observations, as shown in Figure 1. For the different shapes of short skirts, dresses, and shirts made by three-dimensional cutting, the highest score is the short skirt, and the lowest score is the shirt. Three-dimensional cutting combines the advantages of plane cutting and three-dimensional cutting. It has both the simplicity and practicality of plane cutting and the beautiful appearance of three-dimensional cutting. It has strong market development efforts. In the software operation of three-dimensional cutting, the virtual mannequin is used to build the overall shape of the garment on the mannequin, and then draw the garment structure lines on the three-dimensional garment outline, and use the three-dimensional garment structure lines to generate a flat pattern of garment pieces. Therefore, in the subjective review, the scores of the three clothing items are relatively high. The shape design and the development of the flat shape are relatively time-saving and labor-saving, and the fit is more suitable for the human body. The structure line of the three-dimensional skirt is simple, and the lines can be completed smoothly. Therefore, the overall shape is more graceful than dresses and shirts. Shirts have more structure lines, and there are more curves in the neckline and collar. Short skirt design takes twice as long to complete. The 3D cutting software is simple and convenient to operate, saving time, effort, and resources. Therefore, a large number of enterprises are attracted to introduce virtual reality technology to assist clothing design and become a new model of computer-aided clothing design to successfully promote the transformation of enterprise employment forms and the improvement of enterprise production efficiency. As shown in Table 1, three different human body models are measured.

Through the comparative analysis of the skirt shape, dress shape, and shirt shape in Figure 12, it can be seen that most people’s rational consciousness still tends to be more convenient and three-dimensional. Among them, three-dimensional tailoring has objective advantages and exerts that in order to meet the needs of body tailoring and display figure, at the same time, it has the demand for the looseness of flat cutting. Customers with different needs can make clothing with high flexibility and abandon the complicated operation of three-dimensional cutting. A trial-made white-grey cloth saves time and materials, removes the fixed formulation of the plane structure to make the board, and adopts the virtual trial-on-the-board model, which meets people’s higher requirements for computer-aided design in the new era, making computer-aided design deep into all levels of clothing design, laying the advantages of computer technology on the desktop, making clothing companies aware of the effects of computer-aided design, saving resources for the society, and improving economic and social benefits. Figure 13 shows the virtual fitting system.

4.2. *How to Measure Hip Circumference.* Hip circumference refers to the horizontal circumference of the hip measured at the fullest part of the hip when the subject is standing upright. Therefore, as a plane that passes through the fullest part of the buttocks and is parallel to the horizontal plane XY of the system, cut this plane with the human body model, and the intersection formed by the cutting is the hip line. The method of selecting the fullest part of the buttocks is as follows. First, determine the coordinate axis of the human body model image; the X-axis is the thickness direction of the human body, the Y-axis is the front width direction of the human body, and the Z-axis is the height direction of the human body. Second, make a plane parallel to the system plane YZ to make this plane gradually approach the buttocks of the human body model. When

TABLE 1: Comparison table of body shape data between the original mannequin and the new mannequin (unit: cm).

Measuring part	Primitive mannequin	Mannequin A	Mannequin B
Height	160.54	165.94	160.54
Chest circumference	84.42	87.50	84.72
Waistline	66.41	69.48	94.31
Hips	91.85	91.67	91.86
Shoulder width	29.51	36.98	29.51
Upper arm circumference	26.39	26.38	26.39
Thigh circumference	55.44	51.55	55.44
Calf circumference	34.54	35.77	34.54
Thigh length	34.77	36.68	34.77
Calf length	39.69	42.15	39.69

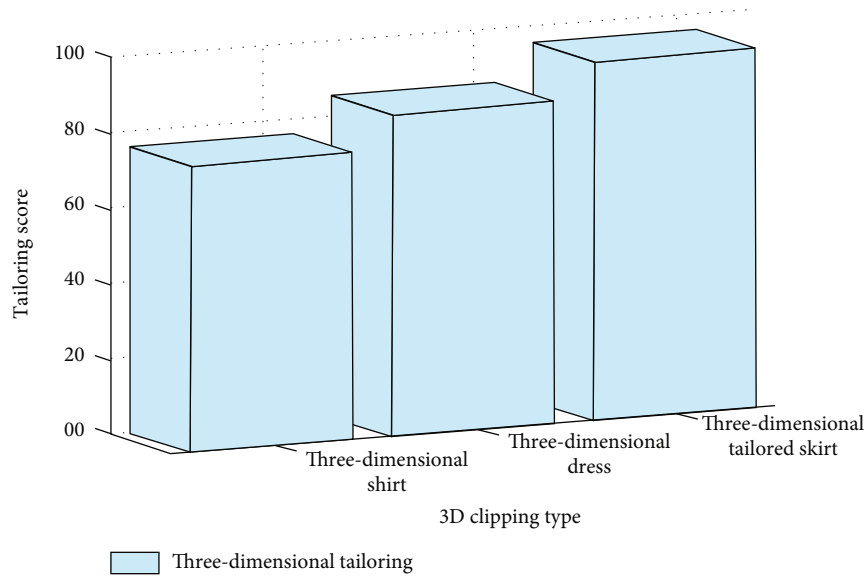


FIGURE 12: Comparison between three-dimensional cutting and different clothing shapes.

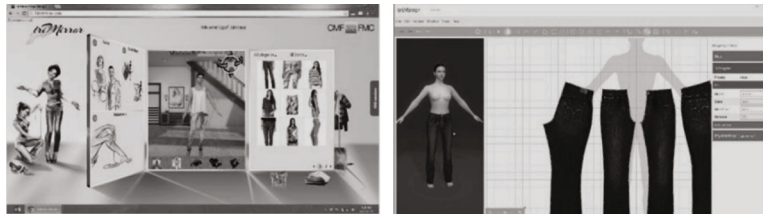


FIGURE 13: Online virtual fitting system.

the plane and the buttocks of the human body appear for the first intersection, this point is the fullest point of the buttocks of the human body model. The line of intersection of the human body model is the hip circumference, and the circumference of this line of intersection is the length of the human hip line. Now, take the example of finding the fullest point of the human left buttocks. First, mesh the image of the left buttocks of the human body; that is, cut the left buttocks. Here, we make 28 cross-sections, each with an interval of 3 mm, and 25 vertical sections, each with an inter-

val of 3 mm. The method to prove that the first point of intersection between the flat and the human buttocks is the fullest point of the buttocks of the mannequin is similar to that of the front breast point. The coordinates of the intersection of the plane and the buttocks and the coordinates of the surrounding points can be expressed by software. The intersection point of the buttocks and the surrounding points are the intersection points of the warp-to-grids after the meshing and cutting of the mannequin. For the convenience of research, here, we take the coordinates of the

TABLE 2: Point coordinates.

11 point coordinates of the intersection point of the hip and its surroundings							
Point name	X-axis	Y-axis	Z-axis	Point name	X-axis	Y-axis	Z-axis
1	121.71	45.402	41.369	7	136.867	46.402	43.226
2	129.207	47.402	43.351	8	130.176	53.402	46.350
3	123.456	49.402	45.324	9	125.371	45.402	42.382
4	129.56	52.402	40.252	10	129.864	47.402	45.622
5	126.926	45.402	42.321	11	135.121	49.402	42.328
6	130.261	43.402	46.346	12	133.013	51.402	49.351

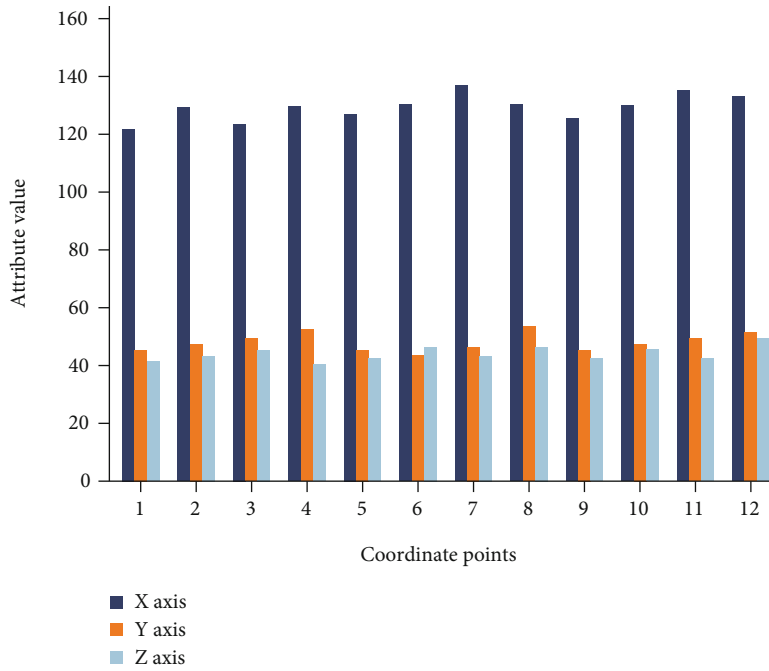


FIGURE 14: Comparison of hip data under virtual reality technology.

intersection point of the buttocks and the coordinates of 11 points around it as an example. The coordinates of each point are shown in Table 2. The comparison of hip data under virtual reality technology is shown in Figure 14.

It can be seen from the coordinate positions of these points that the larger the X-axis coordinates of these points, the closer the plane parallel to the system plane YZ. Then, the point with the largest X-axis of these points is the earliest point that is parallel to the system plane YZ.

**4.3. Design of the Virtual Clothing Contour.** The outline of virtual clothing is formed by connecting key points of clothing and characteristic line segments. This article is to design a simple and loose top T-shirt. You need to get the data of the collar width, clothing length, and hem width first. First, read the 3DS file of the human body model derived from the modeling software through the program, obtain the human body model, and extract the neck points and hip bone points of the human body model. The coordinate values of the neck point and hip bone point are shown in Table 2. Then, calculate the human body’s neck width, the

length from the hip bone to the neck, and the hip bone width. The neck width is obtained by calculating the difference between the X-coordinates of the left and right neck points, and the length from the hip bone to the neck is calculated by calculating the Y-coordinate value of the hip bone point, and the difference in the Y-coordinate value of the hip bone point is obtained, and the hip bone width is obtained by calculating the X-coordinate difference between the left and right hip bone points. Using these body characteristic parameter values as a reference, design the T-shirt’s collar width, dress length, and hem width. Then, use the coordinates of these two feature points as a reference, set the coordinates of key points of clothing, connect these key points through line segments, and make the initial contour of the clothing, that is, the piece of clothing. Mark points 1-8 as key points of clothing. The coordinate values of the points are shown in Table 3. Because the design is a loose-fitting T-shirt, the clothing size in Table 3 is slightly larger than the corresponding body characteristic parameter value in Table 4. The line segments here include straight and curved segments. The curved segments use Bezier curves to

TABLE 3: Coordinate values of key points of clothing pieces.

Key point	X	Y	Z
Key point 1	0.126	0.484	0.214
Key point 2	0.104	0.368	0.328
Key point 3	0.236	0.471	0.635
Key point 4	0.525	0.516	0.469
Key point 5	0.167	0.125	0.256
Key point 6	0.323	0.436	0.447
Key point 7	0.187	0.417	0.105
Key point 8	0.125	0.238	0.269

TABLE 4: Coordinate values of human body feature points.

Feature points	X	Y	Z
Left neck point	0.03934	0.642265	0.0838154
Right neck point	0.05934	0.452265	0.0298154
Left hip point	0.08249	0.725994	0.0068023
Right hip point	0.0827933	0.035994	0.0258023

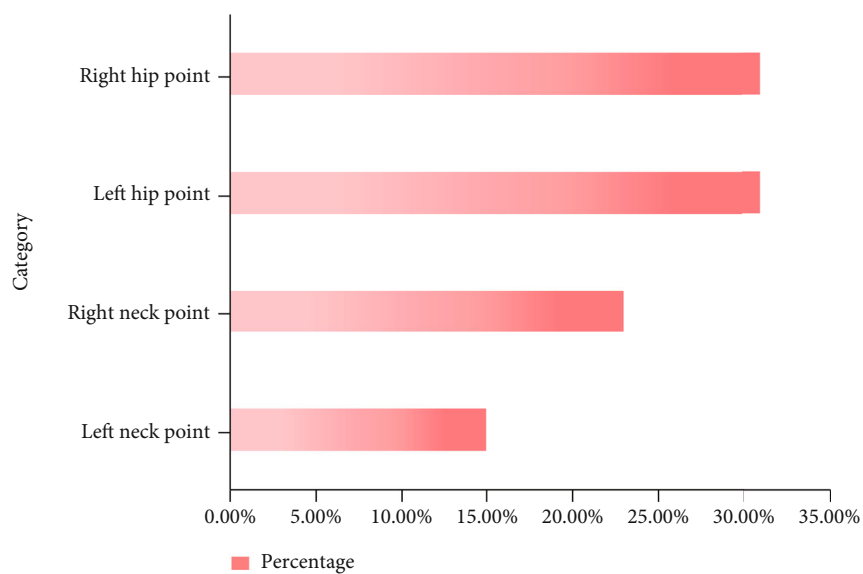


FIGURE 15: Percentage of human body feature point coordinate values.

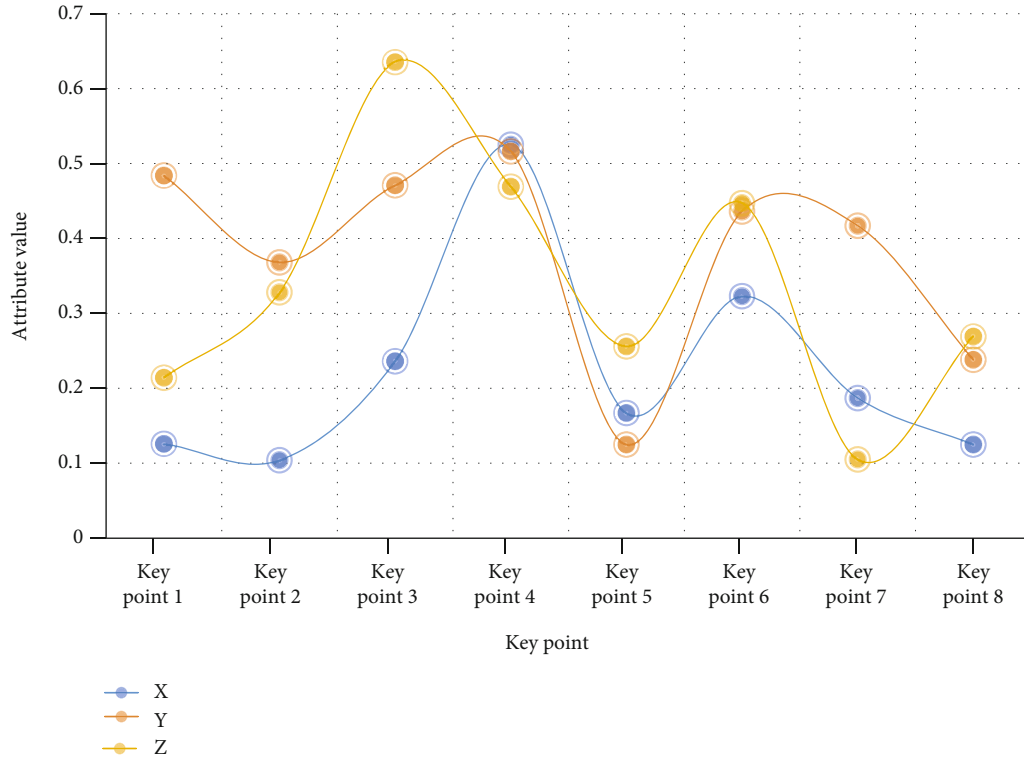


FIGURE 16: Coordinate values of key points of clothing pieces.

construct the neckline and cuffs of the clothing, and the rest are constructed with straight segments. The percentage of the coordinate values of the feature points of the human body is shown in Figure 15. The coordinate values of key points of clothing pieces are shown in Figure 16.

It can be seen from Table 3 and Figure 16 that the Z-coordinate value of the key point is determined according to the depth value of the human body. It is found that as long as  $|Z| > 0.042547$  is satisfied, the clothing and the human body part can be prevented from crossing when the clothing matches the human body. In this article, in order to prevent large deviations in the garment stitching process, if it is the front piece of the garment, take  $Z = 0.06$ . If it is the back film, take  $Z = -0.06$ .

### 5. Conclusions

This article explores 3D clothing design through a combination of the multiple tool software and virtual reality development and display system, which breaks through many limitations of conventional 3D clothing design and provides a richer means of human-computer interaction. In this technology, the user can observe the wearing effect of the clothing from multiple angles and can interactively change the clothing collocation and fabric texture of the characters in the scene, which better achieves the purpose of three-dimensional clothing design. The 3D platform created in this paper provides good basic functions for 3D operations and views. The user interface content is arranged reasonably, concisely, and conveniently. The icons and buttons are arranged regularly, and the screen is simple and vivid. Users

can directly click various tool buttons on the interface to achieve corresponding functions. The measurement method used in this paper is faster and more accurate than traditional measurement methods.

This article applies the concept of virtual reality technology to clothing design to form a clothing virtual reality experience. The clothing virtual reality implements various driving and linkage operations on the clothing parameterized model. Feature-based clothing modeling technology provides more methods for clothing modeling while also expanding the traditional feature modeling methods. The three driving methods of size, sketch interaction, and human body provide examples for the integrated application of multiple deformation methods for the same model. The linkage method based on hierarchical linkage and dimensional linkage is the whole process—multidimensional and multilevel parameterization of the product design exploration.

In this paper, 5G virtual reality technology is applied to 3D clothing design work so that designers can imitate the real environment, interact with the computer in 3D, and effectively carry out 3D free clothing design. This paper observes the three-dimensional effect of the design garment pieces in the virtual reality environment. The three-dimensional interactive ball can realize the spatial control of three-dimensional objects with 6 degrees of freedom, and it is through it that the design of three-dimensional virtual clothing is realized. Using the three-dimensional space ball as a means of three-dimensional interaction with the computer to directly generate three-dimensional virtual clothing is an innovation. Although the current function of the 3D garment piece design system is not perfect, it has

been proved that this method itself is an effective method to generate 3D virtual clothing.

## Data Availability

This article does not cover data research. No data were used to support this study.

## Conflicts of Interest

The author declares that they have no conflicts of interest.

## Acknowledgments

This study was supported by the Hunan Education Science “13th Five-Year Plan” 2020 Project (xjk20bzy022), with the subject name “Research on the construction of art design specialty group in Hunan Higher Vocational Colleges Based on 1 + X certificate system.”

## References

- [1] S. Bobrova, T. Lelina, N. Beskin, V. Bezsmertna, and L. Halavska, “The use of 3D geometric models in special purpose knitwear design and predicting of its properties,” *Vlákna a Textil (Fibres and Textiles)*, vol. 25, no. 2, pp. 19–26, 2018.
- [2] Z. Dong, G. Jiang, G. Huang, and H. Cong, “A web-based 3D virtual display framework for warp-knitted seamless garment design,” *International Journal of Clothing Science and Technology*, vol. 30, no. 3, pp. 332–346, 2018.
- [3] X. J. Zhu, X. Wu, X. Shi, and B.-g. Xu, “Framework of personalized clothing visualization,” *International Journal of Clothing Science and Technology*, vol. 29, no. 3, pp. 417–426, 2017.
- [4] X. J. Zhu, H. Lu, and M. Raetsch, “An interactive clothing design and personalized virtual display system,” *Multimedia Tools and Applications*, vol. 77, no. 20, pp. 27163–27179, 2018.
- [5] G. Chen, F. Ma, Y. Jiang, and R. Liu, “Virtual reality interactive teaching for Chinese traditional Tibetan clothing,” *Art Design & Communication in Higher Education*, vol. 17, no. 1, pp. 51–59, 2018.
- [6] J. Sun, Q. Cai, T. Li, L. Du, and F. Zou, “Body shape classification and block optimization based on space vector length,” *International Journal of Clothing Science and Technology*, vol. 31, no. 1, pp. 115–129, 2019.
- [7] Z. Kang, F. Wang, and Udayraj, “An advanced three-dimensional thermoregulation model of the human body: development and validation,” *International Communications in Heat and Mass Transfer*, vol. 107, pp. 34–43, 2019.
- [8] L. Yang, Q. Huang, X. Song, M. Li, C. Hou, and Z. Xiong, “Girth measurement based on multi-view stereo images for garment design,” *IEEE Access*, vol. 8, pp. 160338–160354, 2020.
- [9] J. L. Maples-Keller, B. E. Bunnell, S. J. Kim, and B. O. Rothbaum, “The use of virtual reality technology in the treatment of anxiety and other psychiatric disorders,” *Harvard Review of Psychiatry*, vol. 25, no. 3, pp. 103–113, 2017.
- [10] J. Q. Coburn, I. J. Freeman, and J. L. Salmon, “A review of the capabilities of current low-cost virtual reality technology and its potential to enhance the design process,” *Journal of Computing and Information Science in Engineering*, vol. 17, no. 3, 2017.
- [11] Y. Sang, Y. Zhu, H. Zhao, and M. Tang, “Study on an interactive truck crane simulation platform based on virtual reality technology,” *International Journal of Distance Education Technologies*, vol. 14, no. 2, pp. 64–78, 2016.
- [12] Y. Zhang and X. L. Ma, “Research on image digital watermarking optimization algorithm under virtual reality technology,” *Discrete & Continuous Dynamical Systems*, vol. 12, no. 4-5, pp. 1427–1440, 2019.
- [13] Y. Ding, Y. Li, and L. Cheng, “Application of Internet of Things and virtual reality technology in college physical education,” *IEEE Access*, vol. 8, pp. 96065–96074, 2020.
- [14] Z. Cai, Z. He, X. Guan, and Y. Li, “Collective data-sanitization for preventing sensitive information inference attacks in social networks,” *IEEE Transactions on Dependable and Secure Computing*, vol. 15, no. 4, pp. 577–590, 2018.
- [15] Z. Cai and Z. He, “Trading private range counting over big IoT data,” in *2019 IEEE 39th International Conference on Distributed Computing Systems (ICDCS)*, pp. 144–153, Dallas, Texas, 2019.
- [16] Z. Lv, X. Li, and W. Li, “Virtual reality geographical interactive scene semantics research for immersive geography learning,” *Neurocomputing*, vol. 254, pp. 71–78, 2017.
- [17] Z. Lv, D. Chen, R. Lou, and H. Song, “Industrial security solution for virtual reality,” *IEEE Internet of Things Journal*, vol. 8, pp. 6273–6281, 2020.
- [18] L. Li, F. Yu, D. Shi et al., “Application of virtual reality technology in clinical medicine,” *American Journal of Translational Research*, vol. 9, no. 9, pp. 3867–3880, 2017.
- [19] C. Donghui, L. Guanfa, Z. Wensheng, L. Qiyuan, B. Shuping, and L. Xiaokang, “Virtual reality technology applied in digitalization of cultural heritage,” *Cluster Computing*, vol. 22, no. S4, pp. 10063–10074, 2017.
- [20] Y. Huang, Q. Huang, S. Ali, X. Zhai, X. Bi, and R. Liu, “Rehabilitation using virtual reality technology: a bibliometric analysis,” *Scientometrics*, vol. 109, no. 3, pp. 1547–1559, 2016.
- [21] J. Yang, C. Wang, B. Jiang, H. Song, and Q. Meng, “Visual perception enabled industry intelligence: state of the art, challenges and prospects,” *IEEE Transactions on Industrial Informatics*, vol. 17, pp. 2204–2219, 2021.
- [22] Z. Liang and R. Shuang, “Research on the value identification and protection of traditional village based on virtual reality technology,” *Boletín Tecnico/Technical Bulletin*, vol. 55, no. 4, pp. 592–600, 2017.
- [23] T. N. Chen, X. T. Yin, X. G. Li et al., “Application of 3D virtual reality technology with multi-modality fusion in resection of glioma located in central sulcus region,” *Zhonghua Yi Xue Za Zhi*, vol. 98, no. 17, pp. 1302–1305, 2018.
- [24] L. Zeming, “Design and implementation of a Korean language teaching system based on virtual reality technology,” *Agro Food Industry Hi Tech*, vol. 28, no. 1, pp. 2156–2159, 2017.
- [25] Y. Sang, Y. Han, Y. Dai, and F. Li, “The development of an interactive automatic tool changer system based on virtual reality technology,” *International Journal of Multimedia & Ubiquitous Engineering*, vol. 11, no. 9, pp. 329–342, 2016.
- [26] H. Guo, “Application of virtual reality technology in swimming teaching,” *Applied Mechanics & Materials*, vol. 11, no. 11, pp. 1230–1234, 2016.



- [27] I. F. Akyildiz, S. Nie, S. C. Lin, and M. Chandrasekaran, "5G roadmap: 10 key enabling technologies," *Computer Networks*, vol. 106, no. 4, pp. 17–48, 2016.
- [28] P. Salva-Garcia, J. M. Alcaraz-Calero, R. M. Alaez, E. Chirivella-Perez, J. Nightingale, and Q. Wang, "5G-UHD: design, prototyping and empirical evaluation of adaptive ultra-high-definition video streaming based on scalable H.265 in virtualised 5G networks," *Computer Communications*, vol. 118, pp. 171–184, 2018.
- [29] S. Savazzi, S. Sigg, F. Vicentini, S. Kianoush, and R. Findling, "On the use of stray wireless signals for sensing: a look beyond 5G for the next generation of industry," *Computer*, vol. 52, no. 7, pp. 25–36, 2019.
- [30] Y. Wang, P. Li, Y. Liu, Y. Sun, and L. Su, "Variable snap-off study for 3D additive screen printing," *International Journal of Clothing Science and Technology*, vol. 32, no. 3, pp. 430–445, 2020.
- [31] M. K. Yoon, Y. J. Nam, and W. Kim, "Classifying male upper lateral somatotypes using space vectors," *International Journal of Clothing Science and Technology*, vol. 28, no. 1, pp. 115–129, 2016.
- [32] X. Yao, J. Wang, S. P. Ashdown, S. Luo, and H. Shi, "Analysis of females' preferences for buttock shapes with different ethnic backgrounds," *International Journal of Clothing Science and Technology*, vol. 28, no. 5, pp. 600–611, 2016.
- [33] S. Wang, X. Wang, and Y. Wang, "Effects of clothing ease and body postures on the air gap and clothing coverage," *International Journal of Clothing Science & Technology*, vol. 31, no. 4, pp. 578–594, 2019.